First Experimental Evidence for Quantum Echoes in Scattering Systems

C. Dembowski,[1] B. Dietz,[1] T. Friedrich,[1] H.-D. Gräf,[1] A. Heine,[1] C. Mejía-Monasterio,[2]
M. Miski-Oglu,[1] A. Richter,[1] and T. H. Seligman[3,4]

[1]*Institut für Kernphysik, Technische Universität Darmstadt, D-64289 Darmstadt, Germany*
[2]*Center for Nonlinear and Complex Systems, 22100 Como, Italy*
[3]*Centro de Ciencias Físicas, UNAM, Mexico*
[4]*Centro Internacional de Ciencias, Cuernavaca, Mexico*
(Received 10 February 2004; published 23 September 2004)

A self-pulsing effect termed quantum echoes has been observed in experiments with an open superconducting and a normal conducting microwave billiard whose geometry provides soft chaos, i.e., a mixed phase space portrait with a large stable island. For such systems a periodic response to an incoming pulse has been predicted. Its period has been associated with the degree of development of a horseshoe describing the topology of the classical dynamics. The experiments confirm this picture and reveal the topological information.

Billiards have served as a paradigm for chaotic dynamics ever since the pioneering work of Sinai [1]. Flat microwave cavities of a shape corresponding to billiards have been extensively used to detect quantum signatures of classical chaos and have served as analog systems for properties of atoms, nuclei, and molecules [2–5]. More recently these analogies became much closer with the discussion of nanostructures such as quantum dots and quantum wires [6,7]. While work first concentrated on closed billiards for the study of spectra and wave functions [2,3], more recently interest focused on scattering systems. On one hand, antennas were considered as open channels [8–11] and, on the other hand, outright open billiards, e.g., billiards connected to waveguides [12–16] have been studied. In the latter case the waveguides make these systems rather complicated. Recently there has been a proposition [17–19] that open scattering systems with a well defined finite interaction region may display a self-pulsing effect called quantum echoes [20], if we excite a system which has a very large stable island in phase space with a short pulse. In billiards such situations can be reached if the connection to the exterior region occurs through fairly narrow necks. If the classical scattering dynamics is chaotic, we usually find a chaotic layer which surrounds the stable island in phase space. The scattering echoes will yield information on the characteristic structure of this layer [21]. Importantly, this is also true if the observation is of wave mechanical type. In this sense our experiment is an approach to the inverse chaotic scattering problem [17].

In order to observe the predicted echoes and measure their period, experiments were performed using flat resonators both at room temperature and in a superconducting state at 4.2 K. The data were taken for continuous input at fixed frequencies covering a range from 0 to 20 GHz, and a Fourier transform of these results yields the response to a short incoming pulse that we require. We

first discuss the geometry of the resonator as well as the location of the antennas that will be used to feed or detect the microwaves. Next we consider a surface of section of the classical motion within this geometry, in order to verify that we fulfill the conditions to obtain echoes. The relation of the echo period to the classical scattering dynamics will be touched upon, and then we proceed to show and discuss the experimental results.

The geometry of the billiard (Fig. 1) is given by a Gaussian as an upper boundary and a parabola as a lower one,

$$y_u(x) = \lambda \exp\left(-\frac{\alpha x^2}{\lambda^2}\right) \quad \text{and} \quad y_l(x) = \lambda\left(\beta - \frac{\gamma x^2}{\lambda^2}\right). \quad (1)$$

The parameters have been chosen as $\alpha = 0.161$, $\beta = 0.2$, and $\gamma = 0.1$, and $\lambda = 5$ cm is a scaling factor. The billiard extends from $x = -25$ cm to $x = 25$ cm and shows a stable fundamental periodic orbit along its symmetry axis at the middle and two unstable ones in the necks
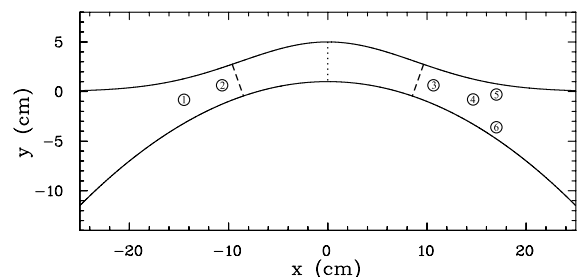

FIG. 1.   The open billiard used in this work possesses a stable orbit (dotted line) and two unstable periodic orbits (dashed lines) at the necks. Between the unstable orbits, a wave packet can get trapped. The circles indicate the positions of the antennas (labeled by numbers from left to right) used in the microwave experiment.

where the distance between both boundaries is minimal. In the following the part of the billiard between the unstable orbits is called the interior, and the complement the exterior. The circles in Fig. 1 refer to the positions of the antennas. They are located in the exterior of the billiard. Note that a direct transmission of microwaves through the billiard is not possible.

The Poincaré section of the billiard, which has been obtained from a classical ray tracing simulation of particles in order to illustrate the classical trajectories, is shown in Fig. 2. Each point corresponds to a reflection on the lower boundary, where the Birkhoff coordinates refer to the arc length of the point of impact on the boundary and to the tangential component of the momentum with respect to that boundary. One clearly can see an island of stability which has been obtained from trajectories confined to the interior of the billiard. Its center is an elliptic fixed point corresponding to the fundamental stable orbit. A chaotic layer which surrounds the island results from the exterior region; here we find two hyperbolic fixed points, associated with the two unstable orbits. This situation is generic. It corresponds to the one of a pendulum with a perturbation [22]. Here the scattering trajectories take the place of the revolutions of the pendulum while the oscillatory island remains in place. Because of the perturbation, the separatrix is deformed mainly near the two unstable points, resulting in a chaotic layer.

Particles have a characteristic time for one revolution about the stable island. Each time they approach one of the necks of the billiard, they have a chance to escape. Thus from the exterior regions particles can be observed to leave the interior region periodically at certain times after an emission of a particle ensemble, and classical echoes arise.

The rectangular area around the right-hand side (rhs) unstable fixed point displays a complicated structure of tendrils. This is a typical signature of horseshoe construction (for details, see [21]) underlying the dynamics of the system. This horseshoe is characterized by a parameter β, which gives a hint on the degree of chaoticity of the system and can be obtained from the lengths and widths of the tendrils. The parameter β is related to the period T of the echoes as

$$T = \tau(-2\log_3\beta + 3/2). \qquad (2)$$

The quantity τ is the average time between two reflections at the lower boundary. It can be sufficiently estimated from the size of the scattering center, i.e., from the length of the stable orbit in our billiard. The development parameter of the horseshoe can be expressed as $\beta = 3^{-8}$. In this conventional notation, the base corresponds to the number of outcoupling channels plus one for the interior region. This yields an echo period of $T = 4.67$ ns, which matches very well with the result obtained from the classical simulation of $T = 4.67 \pm 0.62$ ns. The error results from the finite width of the echoes.

The quantum billiard was studied in the experiment using a microwave cavity sufficiently flat so that the vectorial Helmholtz equation for the electromagnetic field is reduced to the scalar Helmholtz equation for the electric field alone which is equivalent to Schrödinger's equation for a particle in a quantum billiard [2,3]. The billiard was constructed from lead covered copper plates as in [23].

Measurements of the transmission parameters S_{ij} through the cavity, where i and j denote a pair of antennas, have been performed for the billiard at room temperature in open air as well as in the superconducting state when the billiard has been put into a copper box evacuated and cooled down to 4.2 K. In order to guarantee
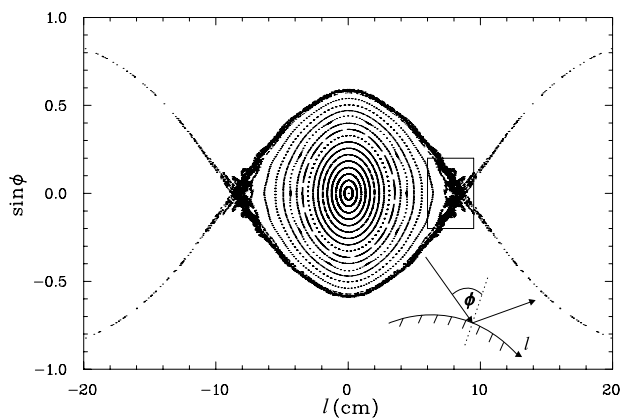

FIG. 2.   A Poincaré section of the open billiard consists of a stable island and a surrounding chaotic layer with two hyperbolic points. Each point in the section corresponds to the angle of reflection ϕ and arc length l of a point of reflection at the lower boundary of the billiard. The rectangle enclosing the rhs unstable fixed point shows a heteroclinic structure.
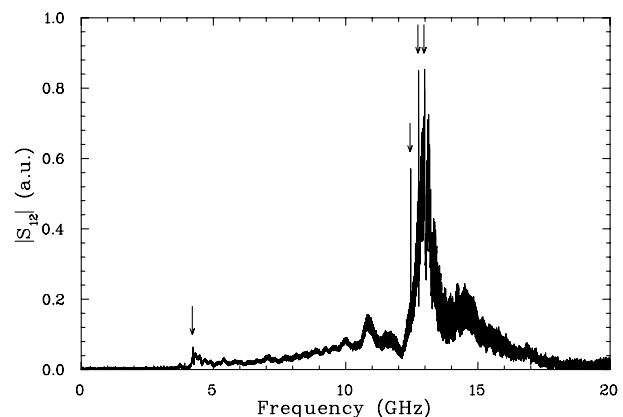

FIG. 3.   Spectrum obtained from a measurement of the transmission parameter $|S_{12}|$ between antennas 1 and 2 in the superconducting resonator. The arrows mark four narrow resonances. More of those are detected with other antenna combinations. All sit on top of a continuous spectrum.

the openness in the latter case, the openings of the billiard as well as parts of the box were stuffed with a urethane based microwave absorber EMC CRAM-AR (HP). By this foamlike material an attenuation of microwave power by 2 orders of magnitude was achieved for frequencies larger than 6 GHz. Below this frequency, the absorption is not uniform, which turned out not to be a disadvantage, because the measured amplitudes are small in this regime. Furthermore, to show that the use of these absorbers is equivalent to maintain an open system, we performed experiments at room temperature in open air with and without the absorbers. The results coincide.

The measurement consisted of obtaining S-matrix transmission parameters using a vectorial network analyzer HP-8510C. Figure 3 shows a spectrum for $|S_{12}|$ in the superconducting case. The spectrum is continuous, and several sharp resonances are visible. To get the impulse response in the time domain, a Fourier transform was performed on all spectra using a windowed fast-Fourier-transform (FFT) routine. The upper part of Fig. 4 shows the time signals corresponding to the data of Fig. 3, and the inset exhibits the same at much longer times. In the lower part the signal obtained from the same measurement at room temperature is displayed. In both time spectra no transmission is seen below a certain offset time, which reflects the minimum time the signal needs to propagate through both the cables to and from the billiard and the billiard itself. One clearly sees periodic oscillations, which are shown to be the predicted quantum echoes. In some measurements with the superconducting resonator, more than 100 echo periods were identified as can be seen from the inset. In addition, some huge peaks

appear in the time spectra. They are due to standing waves on the cables as has been checked by varying the cable lengths. Thus they are well understood and do not affect the experimental results.

To show that the observed echoes are the ones predicted [17], we first introduced a metal disk into the inner part of the billiard. From a classical point of view, this destroys the stable island in phase space, which is the theoretical basis for the echoes. Indeed the experiment reveals that the echoes disappear (the corresponding figure is not displayed). Second, the model does not only predict echoes to be detected on both sides of the cavity outside the necks, but also that those on the rhs should appear in counter phase to those on the left-hand side. In Fig. 5, two transmission measurements at room temperature are presented. The upper part shows the measured $|S_{23}|$ parameter between antennas 2 and 3 (cf. Fig. 1), while the lower part similarly exhibits $|S_{12}|$. Note that the upper part corresponds to a transmission through the cavity, while the lower part shows a reflection, though measured by a transmission experiment for two antennas at the same side. Comparing the upper and the lower part of the figure we clearly see the predicted counter phase behavior.

We now discuss two important features of the results. First, it is clear (e.g., from Fig. 5) that the period of the echoes gets shorter as a function of time. If we analyze the data for the superconducting cavity (cf. Fig. 4, upper part) we find that the period of the echoes starts at 4.2 ± 0.25 ns and slowly decreases to stabilize near 3.3 ± 0.25 ns. Second, a semilog plot (not displayed) of the same data reveals after roughly ten oscillations an exponential decay of the average intensity over almost two decades.

Both phenomena can be understood in terms of the classical phase portrait (cf. Fig. 2) and the concept of
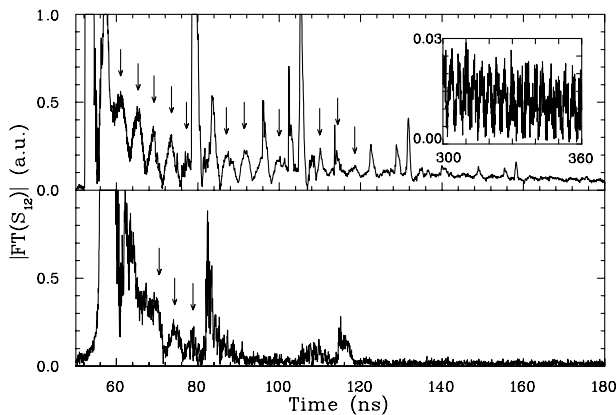

FIG. 4. Time spectra resulting from a FFT of the spectrum in Fig. 3 (upper part) and from the same measurement at room temperature (lower part). The arrows indicate the early visible echoes. The additional large peaks are caused by standing waves on the cables from the rf source to the resonator and from the resonator to the network analyzer. The different offset times in the upper and the lower part are due to different cable lengths. The inset shows echoes at very late times. They could be detected only in the superconducting case.
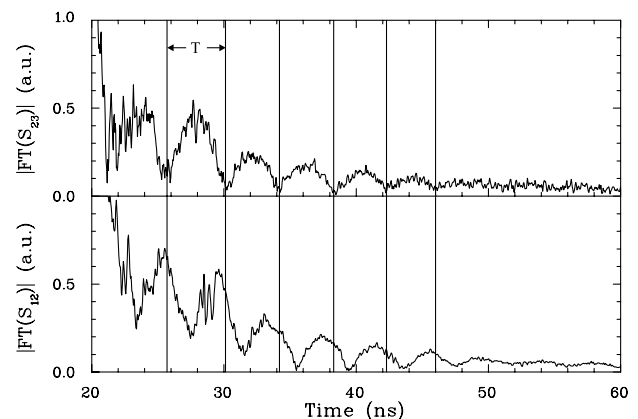

FIG. 5. Comparison of transmission measurements between antennas on different sides (upper part) and on the same side (lower part) of the resonator. A shift of the peaks by about half a period is visible as expected from the classical model. Note the shortening of the echo periods T with time.

dynamical tunneling through integrable areas. As our antennas lie outside the necks no power is injected into the system inside the island. Thus the inside can exclusively be populated by tunneling, while for the chaotic layer tunneling may compete with evolution along classically allowed trajectories. At any rate the intensity on average drops with increasing penetration depth into the island. The time for emission from the chaotic layer and from inside the island also increases as we receive the signal from deeper layers. From the interior of the island the tunneling decay should be exponential, while we expect both tunneling and direct contributions from the chaotic layer. It is thus quite clear that we receive the outgoing signal and, particularly, the echoes from ever deeper inside the island as time advances. At this point it is important to note that the rotation period of the island in our case decreases from the edge, i.e., from the chaotic layer towards the interior, which is indeed the typical situation, though exceptions can be constructed. Thus we expect shorter periods for the echoes as time advances in accordance with the experiment. The echo period stabilizes and according to this picture we must assume that we are now seeing tunneling from a fixed penetration depth of the island. This implies that the effective barrier is also fixed and that we should see exponential decay, as we indeed do. The asymptotic period can be determined either directly by the innermost states or more probably by the fact that, as we penetrate deeper into the island, the small absorption of the cavity wall that remains even in the superconducting case begins to dominate the emission through the barrier.

This picture indicates that the first echoes stem from the edge of the island or from the chaotic layer, and thus we can invert Eq. (2) to find a value $-\log_3 \beta = 7.1 \pm 1.3$. This is compatible with the value of 8 determined from theory, but probably even the wave packet causing the first echo penetrates the island slightly and therefore has a period which is a little shorter than the classical one.

Summarizing we can conclude the following: We do see the classical echoes predicted and the properties agree qualitatively and quantitatively well with what we expect from classical and semiclassical arguments. It is notable that this agreement is achieved in a regime quite far from the semiclassical limit. It is precisely this fact that allows the waves to penetrate deep into the classically forbidden region and to reveal classical revolution times, which are not accessible in a classical scattering experiment.

[1] Ya. G. Sinai, Russ. Math. Surv. **25**, 137 (1970).
[2] A. Richter, in *Emerging Applications of Number Theory*, The IMA Volumes in Mathematics and Its Applications Vol. 109, edited by D. A. Hejhal *et al.* (Springer, New York, 1999), p. 479.
[3] H.-J. Stöckmann, *Quantum Chaos—An Introduction* (Cambridge University Press, Cambridge, 1999).
[4] S. Sridhar and E. J. Heller, Phys. Rev. A **46**, R1728 (1992).
[5] T. Guhr, A. Müller-Groeling, and H. A. Weidenmüller, Phys. Rep. **299**, 189 (1998).
[6] Y. Imry, *Introduction to Mesoscopic Physics* (Oxford University Press, Oxford, 2002).
[7] J. Bürki, R. E. Goldstein, and C. A. Stafford, Phys. Rev. Lett. **91**, 254501 (2003).
[8] H. Alt *et al.*, Phys. Rev. Lett. **74**, 62 (1995).
[9] J. Stein, H.-J. Stöckmann, and U. Stoffregen, Phys. Rev. Lett. **75**, 53 (1995).
[10] H. Alt *et al.*, Phys. Rev. E **55**, 6674 (1997).
[11] R. Schäfer *et al.*, J. Phys. A **36**, 3289 (2003).
[12] E. Doron, U. Smilansky, and A. Frenkel, Phys. Rev. Lett. **65**, 3072 (1990).
[13] Y.-H. Kim *et al.*, Phys. Rev. B **65**, 165317 (2002).
[14] W. Li, L. E. Reichl, and B. Wu, Phys. Rev. E **65**, 056220 (2002).
[15] J. A. Méndez-Bermúdez *et al.*, Phys. Rev. E **66**, 046207 (2002).
[16] G. A. Luna-Acosta, K. Na, and L. E. Reichl, Phys. Rev. E **53**, 3271 (1996).
[17] C. Jung, C. Mejía-Monasterio, and T. H. Seligman, Europhys. Lett. **55**, 616 (2001).
[18] C. Jung *et al.*, New J. Phys. **6**, 48 (2004).
[19] C. Mejía-Monasterio, Ph.D. thesis, University of Mexico (UNAM), 2001, www.cicc.unam.mx/~mejia/thesis.html.
[20] It is essential to note that the quantum echoes we have observed have no relation to the so-called quantum Loschmidt echoes, i.e., the time evolution resulting from the overlap of the eigenstates of two slightly different Hamiltonians; see, e.g., H. M. Pastawski, P. R. Levstein, and G. Usaj, Phys. Rev. Lett. **75**, 4310 (1995); T. Prosen, T. H. Seligman, and M. Znidaric, Prog. Theor. Phys. Suppl. **150**, 200 (2003).
[21] C. Jung, C. Lipp, and T. H. Seligman, Ann. Phys. (N.Y.) **275**, 151 (1999).
[22] A. J. Lichtenberg and M. A. Lieberman, *Regular and Chaotic Dynamics* (Springer, Berlin, 1983).
[23] C. Dembowski *et al.*, Phys. Rev. E **62**, R4516 (2000).